Review

Israel Journal of Chemistry

DOI: 10.1002/ijch.201400178

Protein- and Peptide-directed Approaches to Fluorescent Metal Nanoclusters

Yihui Hu, Wenjing Guo, and Hui Wei*[a]

Abstract: Fluorescent metal nanoclusters (FMNCs), one of the promising functional nanomaterials, have aroused great interest in diverse areas due to their unique characteristics, such as ultrasmall size, high fluorescence, excellent photophysical and chemical stability, good biocompatibility, and tuneable emissions. Many methods have been developed to prepare the FMNCs. Among them, the biomolecule-directed approach, which could produce FMNCs with high water-solubility, good biocompatibility, enhanced fluorescence, and rich surface chemistry for conjugation has attracted enormous attention. In this review, we highlight the substantial progress in protein- and peptide-directed approaches to varieties of FMNCs. The synthetic protocols and potential formation mechanisms are well summarized. Selected key applications, ranging from biological and chemical detection to cellular and *in vivo* imaging, are also discussed. Finally, the current challenges, as well as future perspectives, are briefly discussed. The lessons from these case studies would provide a valuable guide to designing nanomaterials with desired or even personalized functions in the future.

Keywords: bionanotechnology · fluorescent nanoclusters · functional nanomaterials · peptides · proteins · rational design

1 Introduction

Owing to their intrinsically different features, compared with bulk materials, functional nanomaterials[1] exhibit unique properties, and thus, have found broad applications in various areas, from biosensing and bioimaging[2] to electronics and photovoltaics.[3] Among the functional nanomaterials so far developed, the fluorescent ones have received enormous attention, such as in the field of bionanotechnology, due to their unique and fascinating properties.[4] Particularly, when fluorescent nanomaterials are functionalized with biomolecules, they can be explored for a wide range of biosensing and biomedical applications.[5]

Fluorescent metal nanoclusters (FMNCs), usually consisting of several to tens of atoms, are a new subtype of MNCs with promising fluorescent properties.[6] The ultrasmall size of FMNCs (with a diameter usually less than 2 nm) approaches the Fermi wavelength of conduction electrons in metal (e.g., 0.52 nm for Au and Ag, 0.46 nm for Cu, and 0.36 nm for Al), leading to the continuous density of states splitting into discrete energy levels, and thus rendering FMNCs with unique optical, electrical, electrochemical, magnetic, and chemical properties.[6]

Compared with other fluorescent nanomaterials, such as semiconductor quantum dots (QDs), dye-doped nanoparticles (NPs), upconverting NPs, and carbon-based nanomaterials, FMNCs have several remarkable advantages.[7] First, FMNCs are composed of elements with low toxicity (or even no toxicity), endowing them with excellent biocompatibility. Second, FMNCs (specifically the gold-based ones) are usually inert, providing them with good chemical stability. Third, FMNCs also have extraordinary photophysical stability. Fourth, their ultrasmall sizes make them suitable for biolabelling, without disturbing the functions of to-be-labelled bioentities. The ultrasmall sizes also enable them to be easily drained out *in vivo*. Fifth, the fluorescent emissions can be tuned from visible to infrared by changing the size and composition of the FMNCs. Owing to these fascinating features, FMNCs have shown great promise in advancing numerous research fields.

To prepare such FMNCs, lots of synthetic approaches have been developed (Figure 1).[6d,e,8] Recently, extensive efforts have been devoted to developing facile synthetic

[a] Y. Hu, W. Guo, H. Wei
Department of Biomedical Engineering
Aerosol Bioeffects and Health Research Center
College of Engineering and Applied Sciences
Nanjing National Laboratory of Microstructures, Nanjing University
22 Hankou Road
Nanjing
Jiangsu 210093 (P. R. China)
Tel.: (+86) 25-83593272
Fax: (+86) 25-83594648
Homepage: weilab.nju.edu.cn
e-mail: weihui@nju.edu.cn

Supporting information for this article is available on the WWW under http://dx.doi.org/10.1002/ijch.201400178.

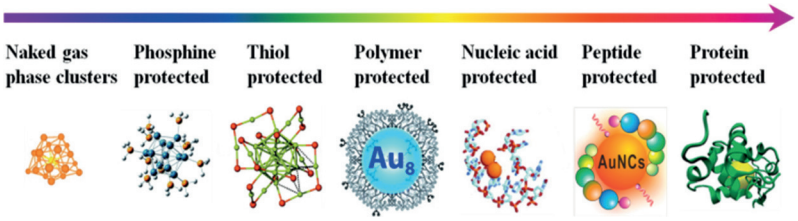

Figure 1. Synthetic approaches to FMNCs using various kinds of ligands (or stabilizing agents). Dendrimers are included in polymers. Unprotected gas phase nanoclusters are also shown for comparison. Reprinted with permission from (left to right): Ref. [83], copyright 2003 American Association for the Advancement of Science; Ref. [84], copyright 2012 Royal Society of Chemistry; Ref. [14b], copyright 2008 American Chemical Society; Ref. [85], copyright 2015 Royal Society of Chemistry; Ref. [6r], copyright 2007 National Academy of Sciences; Ref. [79], copyright 2013 American Chemical Society; Ref. [10], copyright 2010 Royal Society of Chemistry.

approaches for water-soluble FMNCs with much enhanced performance (e.g., improved stability and biocompatibility, and enhanced brightness).[6f–n] Among the many developed methodologies, protein- and peptide-directed synthetic approaches could provide several distinct characteristics, including mild-reaction and green synthetic conditions, controllable sizes and tuneable emissions, self-assembly and programmability, and rich surface chemistry for functionalization, as well as distinctive molecular structures for specific biorecognition (Tables S1–S3).

To highlight the fast progress in the field, this review covers the protein- and peptide-directed approaches to FMNCs, their characterizations, formation mechanisms, and key applications. First, the use of different proteins (such as bovine serum albumin (BSA), lysozyme, and human serum albumin (HSA)) to form several kinds of FMNCs are discussed. Since most studies have been focused on BSA, the BSA-stabilized FMNCs will be intensively discussed. Then, the use of natural, as well as designed, peptides to prepare FMNCs are summarized. Finally, a brief summary and outlook is presented to show the current challenges and future opportunities in designing and synthesizing superior-performance FMNCs. Note: though the definite stoichiometries and structures of a few metal nanoclusters have been established by careful mass spectroscopic analysis and X-ray crystallographic studies,[8i,j] the compositions of the FMNCs tentatively assigned in this review were mainly based on mass spectroscopic analysis, which need to be further confirmed by X-ray crystallographic and other studies.

Due to limited space, only selected examples are discussed. Readers are referred to published reviews for more information (also see the supporting information for a more comprehensive list).[6f–n]

Yihui Hu received her B.S. degree in Chemical Biology from Hengyang Normal University in 2010 and M.S. degree in Analytical Chemistry from Hunan University in 2013. Currently, she is a Ph.D. candidate in Professor Hui Wei's group at Nanjing University. Her research interests are focused on bionanotechnology and cancer nanotechnology.

Wenjing Guo received her B.S. degree in Materials Chemistry from Nanjing University in 2014, where she carried out undergraduate research with Professor Hui Wei. Currently, she is a graduate student in Professor Hui Wei's group at Nanjing University. Her research interests are focused on the design and fabrication of functional nanomaterials for analytical and biomedical applications.

Hui Wei received his B.S. degree from Nanjing University in 2003 and Ph.D. degree from Changchun Institute of Applied Chemistry, Chinese Academy of Sciences in 2008. Currently he is a professor at Nanjing University, working on the design and synthesis of functional nanomaterials and the development of new methodologies for analytical and biomedical applications.

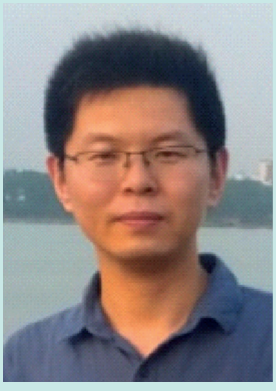

2 Protein-directed Approaches

Proteins, both in solution phase and crystal form, have been extensively studied as templates to prepare various kinds of nanomaterials.[9] Since Xie and co-workers' pioneering work on the synthesis of fluorescent AuNC with BSA (abbreviated as AuNC-BSA), other metal-based NCs have also been successfully prepared, using either BSA or other proteins as the directing and templating re-

agents (Table S1).[8e,10] In this section, the protein-directed approaches to FMNCs, their formation mechanisms, and applications are discussed.

2.1 BSA-directed Approaches

BSA is one of the common structural proteins, containing 35 cysteine (Cys), 21 tyrosine (Tyr), and 3 tryptophan (Trp) residues, out of 583 amino acids in total. The Cys residues form 17 pairs of disulfide bond and one free thiol (from Cys). It is commercially available. By utilizing its reducing capability, mainly from Tyr (and/or Trp), and its templating effect, Xie, as well as others, have demonstrated that BSA could direct the formation of diverse FMNCs (such as Au, Ag, Cu, Pt, and alloy).[8e,11]

2.1.1 AuNCs

Synthetic Protocols and Formation Mechanism. Lots of effort has been dedicated to studying BSA-stabilized AuNCs.[8e,12] Most of this work has adopted the synthetic method developed by Xie *et al.*[8e] Xie's approach was inspired by biomineralization, in which Au ions were first sequestered by BSA, and were then *in situ* reduced, by changing the reaction pH to an alkaline pH (Figure 2a and Figure 4a).[8e] It suggested that positively charged amine groups may be responsible for the uptake of Au ions.[13] Tyr was the main amino acid residue involved in the reduction of Au ions since Tyr's reducing capability could be significantly improved by adjusting the reaction pH above its pK_a (ca. 10).[8e,13] The thiols from Cys and/or amine groups may be involved in stabilizing the formed AuNCs.[13]

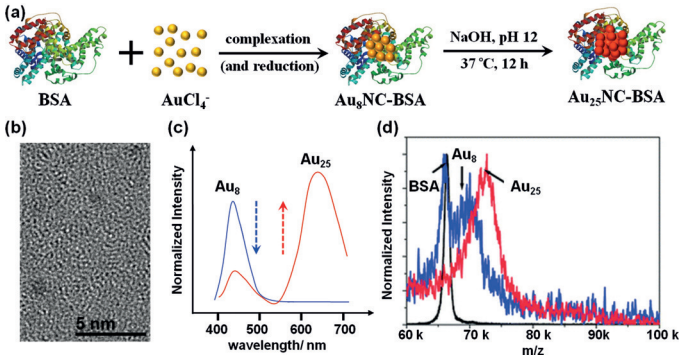

Figure 2. BSA-directed approach to fluorescent AuNC. (a) The synthetic protocol; (b) TEM image; (c) fluorescent spectra; and (d) mass spectra. (b) Reprinted with permission from Ref. [8e]; copyright 2009 American Chemical Society. (d) Adapted with permission from Ref. [12a]; copyright 2012 Royal Society of Chemistry.

The as-prepared AuNC-BSA had a size of around 1 nm under TEM imaging (Figure 2b). It exhibited highly fluorescent emission centred at ca. 640 nm, with a quantum yield (QY) of 6% (Figure 2c). Mass spectroscopy measurements showed the AuNCs had a composition of Au_{25} (Figure 2d). The Au_{25}NC-BSA adopted a structure with a Au_{13} core (in Au^0) and a Au_{12} shell (in Au^+), which was supported by further X-ray photoelectron spectroscopy (XPS) and X-ray absorption spectroscopy (XAS) measurements, and was consistent with the structure of the thiolate protected Au_{25}NC.[8e,14]

Carefully following the reaction process revealed that at least two species were involved during Au_{25}NC-BSA evolution (Figure 2c). Mass spectroscopy measurements suggested that the "blue species" (ca. 440 nm emission) was Au_8NC, while the "red species" (ca. 640 nm emission) was Au_{25}NC (Figures 2c and 2d).[12a] (Note: the "blue species" may alternatively be assigned to the oxidized product of Trp from BSA.[15]) Despite the discrepancy, these studies indicated an evolution as follows: BSA + $HAuCl_4$ → [Au(I)-BSA] (low pH) → Au_8NC-BSA (low to neutral pH) → Au_{25}NC-BSA (high pH). Since the regeneration of free BSA was observed, a possible inter-protein Au atom transfer was suggested to form Au_{25}NC-BSA from Au_8NC-BSA.[12a,15,16]

Usually, centrifugation, dialysis, or lyophilisation was used to purify the as-prepared Au_{25}NC-BSA. However, these methods cannot efficiently separate the free BSA from Au_{25}NC-BSA. Recently, an interesting co-precipitation method was developed to purify Au_{25}NC-BSA.[12b] As shown in Figure 3, the as-prepared Au_{25}NC-BSA could be selectively precipitated out by adding zinc ions at alkaline pH. The subsequent centrifugation and dialysis could remove free BSA and other ions. After redispersion in suitable media, such as a phosphate buffer, the purified Au_{25}NC-BSA, with enhanced fluorescence, was obtained.

A few studies have demonstrated that the size of AuNC-BSA could be tuned by tailoring experimental pa-

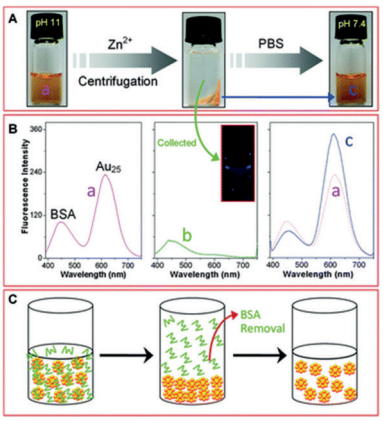

Figure 3. An effective separation process for purifying Au_{25}NC-BSA via co-precipitation with zinc hydroxide on their surfaces. (A) Optical observations during the purification of Au_{25}NC-BSA by the addition of Zn^{2+} solution. (B) fluorescence spectra of (a) the as-synthesized Au_{25}NC-BSA; (b) the supernatant after precipitation; and (c) the purified Au_{25}NC-BSA after being redispersed in buffer. (C) Schematic of the purification of Au_{25}NC-BSA. Reprinted with permission from Ref. [12b]; copyright 2014 Royal Society of Chemistry.

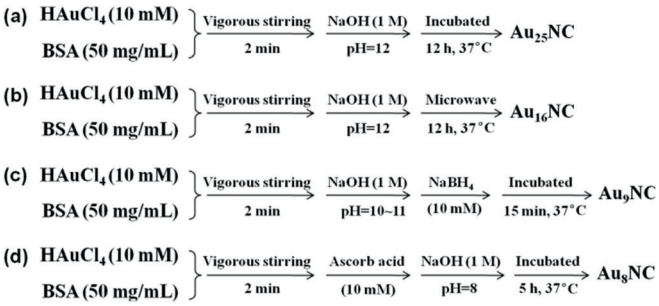

Figure 4. Synthetic protocols for various AuNC-BSA.

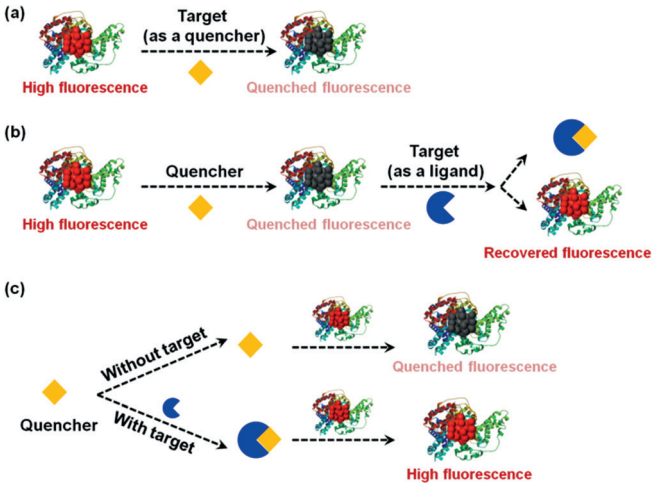

Figure 5. Sensing a variety of targets using AuNC-BSA as a fluorescent probe. (a) Certain targets can selectively quench the fluorescence of the AuNC-BSA, thus providing a "signal-off" protocol for target detection; (b) the quenched fluorescence can be recovered by specific ligands, thus providing a "signal-on" protocol for ligand detection; (c) an alternative protocol for sensing a ligand. (Note: in principle, the AuNC-BSA can be replaced by other FMNCs to construct the above sensing platforms.)

rameters, such as reaction pH, reducing agents, and microwave irradiation (Figure 4).[16,17] For example, using a microwave irradiation-assisted approach, Au_{16}NC-BSA was prepared (Figure 4b), which emitted blue-shifted fluorescence at 604 nm due to its reduced size (as a comparison, Au_{25}NC-BSA emitted at 640 nm).[17b] The synthesis of Au_9NC-BSA and Au_8NC-BSA through the modification of Xie's method (Figures 4c and 4d) was also reported.[16,17] Recently, Xie *et al.* reported a CO-mediated method to synthesize AuNCs with different sizes (i.e., Au_4, Au_8, Au_{10}, Au_{13}, and Au_{25}) in BSA.[18] They showed that the size of AuNCs was mainly dependent on the conformation of BSA. At pH 7.4, the largest AuNC obtained in BSA (with a native conformation) was Au_{13} (though smaller AuNCs, i.e., Au_4, Au_8, and Au_{10}, could be prepared by lower $HAuCl_4$ to BSA ratio). At pH 11, Au_{25} was obtained due to the partially denatured conformation of BSA. However, no fluorescent properties of the synthesized AuNCs were reported.[18]

Applications. AuNC-BSA has been explored for a variety of applications, ranging from metal ion detection and small molecule sensing to immunoassay and bioimaging (Note: the AuNC-BSA used for applications is $AuNC_{25}$-BSA, unless otherwise specified).

As shown in Figure 5a, numerous important targets can selectively quench the fluorescence of the AuNC-BSA, thus providing a "signal-off" protocol for the target detection. These targets include metal ions (Hg^{2+}, Cu^{2+}, and Ni^{2+}),[19] anion ions (CN^-, S^{2-}, NO_2^-, and IO_3^-),[20] small molecules (H_2O_2, glutaraldehyde, vitamin B12, folic acid, ascorbic acid, etc.),[21] drugs,[22] reactive oxygen species (ROS),[23] and proteases.[24]

For example, based on a highly specific metallophilic Hg^{2+}-Au^+ interaction, the fluorescence quenching of $AuNC_{25}$-BSA by Hg^{2+} was explored to selectively detect Hg^{2+}.[19a] It also showed that the AuNCs could be immobilized on a test strip or other substance (such as a sol-gel membrane) for potential routine monitoring of Hg^{2+}.[19a,25] The quenching phenomena of AuNC-BSA by Cu^{2+} and Ni^{2+} were also observed and used for sensing the corresponding metal ions.[19b,c] By etching the core of AuNCs, CN^-, S^{2-}, and IO_3^- could quench the fluorescence and thus be determined.[20] The oxidation-induced quenching of the fluorescence by nitrite, H_2O_2, and ROS was also harnessed to develop "signal-off" sensing systems.[20c,21a,23] For most bioactive small molecules and drugs, they may disturb the interactions between the AuNC core and the BSA ligand, thus leading to fluorescence quenching. Based on such effects, several studies have reported the detection of these molecular targets with AuNC-BSA as the fluorescence probe.[21b–e,22] Proteases can digest the BSA ligand, which results in the destabilization of the AuNC-BSA and the fluorescence quenching. Therefore, proteases (such as trypsin) can also be detected using the approach shown in Figure 5a.[24]

As shown in Figure 5b, when a quencher is complexed by its binding ligand, the quenched fluorescence of AuNC-BSA would be recovered. Or when a quencher is pre-complexed, the formed quencher-ligand complex would not affect the fluorescence of AuNC-BSA (Figure 5c). Based on either the approach, "signal-on" sensing platforms could be developed for such complexing ligands. Compared with the method in Figure 5b, the one in Figure 5c does not affect the interaction between the quencher and the ligand, which would lead to higher "on/off" ratios.

For example, biothiols (such as glutathione (GSH)) have high affinity towards Hg^{2+} and can recover the Hg^{2+}-quenched fluorescence of the AuNC-BSA. By switching the fluorescence on, GSH has been determined, even in living cells.[26] Histidine in biofluids was also successfully detected by turning on the Ni^{2+}-quenched fluorescence of the AuNC-BSA.[19c] Dopamine, an important neurotransmitter, was detected by recovering Cu^{2+}

-quenched fluorescence of the AuNC-BSA in human serum and urine samples.[27] 6-mercaptopurine, a chemotherapy anticancer drug, was also successfully analysed in human serum, based on the method in Figure 5b.[28]

As discussed above, H_2O_2 can quench the fluorescence of AuNC-BSA.[21a] When an oxidase catalysed reaction is combined, the detection of its substrate (Substrate 2 in Figure 6a) with AuNC-BSA could be feasible. Dong's

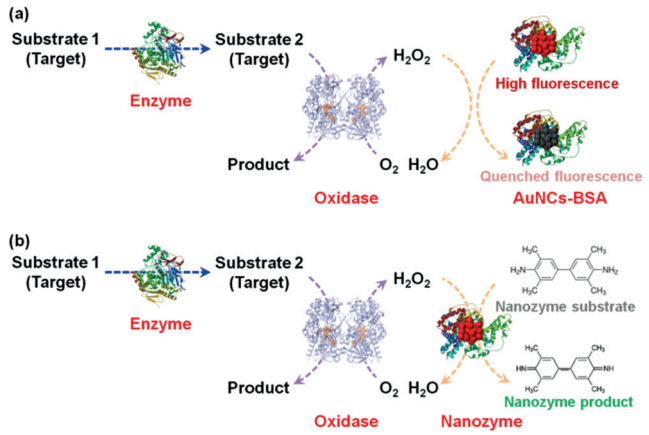

Figure 6. Coupled with enzymatic reactions, more targets can be analysed with AuNC-BSA. (a) Detection based on H_2O_2-induced fluorescence quenching; and (b) detection based on AuNC-BSA as a nanozyme (i.e., a peroxidase mimic). (Note: in principle, the AuNC-BSA can be replaced by other FMNCs to construct the above sensing platforms.)

group reported a glucose detection system by coupling glucose oxidase with the AuNC-BSA. By monitoring the fluorescence decrease, the glucose amounts in human serum were determined, which matched very well with the results measured by the hospital.[21a] As shown in Figure 6a, when another enzyme is introduced and coupled, its corresponding substrate (Substrate 1) can also be detected. For example, acetylcholine was detected in human blood by coupling acetylcholinesterase with choline oxidase and the AuNC-BSA.[29] The method showed excellent selectivity against dopamine, ascorbic acid, and glucose.

Besides quenching effects, a few substances exhibited enhancing effects on the fluorescence of AuNC-BSA. For example, based on Ag^+-induced fluorescence enhancement of Au_{16}NC-BSA, concomitant with emission blue shift, selective detection of Ag^+ was reported.[17b] The enhancement was attributed to the formation a new Au/Ag alloy shell.[17b,30] By exploiting the enhancing effects, F^- and Cys were also detected, respectively.[31]

Nanozymes are newly developed nanomaterials with enzyme like activities.[32] Two groups showed that AuNC-BSA exhibited interesting peroxidase mimicking activity.[33] As shown in Figure 6b, when the peroxidase mimicking activity of the AuNC-BSA is combined with an enzymatic reaction, the corresponding substrate can be assayed. Using such an approach, xanthine levels in urine and serum were determined.[33a] In principle, the method shown in Figure 6 could also be used for screening enzyme inhibitors.

When the AuNC-BSA is conjugated to an antibody, they can be used for immunoassay, as demonstrated by Zhu *et al.*[34] They developed a sandwich-based immunoassay for the determination of the cancer biomarker, neuron-specific enolase (NSE).[34a] The AuNC-BSA was incorporated within porous $CaCO_3$ microspheres to form hybrid materials, which were then further conjugated with a detection antibody for the immunoassay. The proposed assay was highly sensitive and amounts as low as 2.0 pg/mL of NSE were detected.

Electrochemiluminescence (ECL), the luminescence electrochemically triggered on an electrode, has been used as a highly sensitive analytical method for the determination of many important analytes.[35] Recent studies showed that AuNC-BSA also exhibited interesting ECL behaviours.[36] Chen *et al.* found that the AuNC-BSA exhibited ECL with triethylamine as a coreactant at 1.45 V (vs Ag/AgCl in 3 M KCl) on a Pt electrode.[36b] Pb^{2+} detection was accomplished by selectively quenching the ECL. Zhu *et al.* reported a cathodic ECL of the AuNC-BSA in the presence of $S_2O_8^{2-}$ at −1.0 to −1.5 V (vs saturated calomel electrode) on an indium tin oxide electrode.[36a] Dopamine detection was achieved by increasing the ECL.

Due to the sensitivity of BSA conformation to the temperature, the fluorescence of the AuNC-BSA is also affected by temperature.[37] Interesting, it was found that the thermally induced fluorescence quenching of the AuNC-BSA was irreversible. However, when pre-denatured BSA (dBSA) was used to synthesize the AuNC, the fluorescence of the AuNC-dBSA exhibited fully reversible response to temperature changes between 10 and 45 °C. Thus, AuNC-dBSA may be used for cellular temperature tracking.[37a]

Great interest has been devoted to studying AuNC-BSA as a potential contrast agent for cellular and *in vivo* imaging, as well as imaging-guided drug delivery and therapy.[38]

AuNC-BSA is ideal for optical imaging, due to its near infrared (NIR) emission, which has deeper penetration depth and can avoid interference from other biomolecules. Recently, it was shown that the background fluorescence signals could be further inhibited by collecting the emission of long-lived AuNC-BSA 50 ns after excitation.[38a] Wang *et al.* found that the AuNC-BSA could specifically target HER-2 over-expressed breast cancer lines (such as SK-BR3), as well as tumour tissue, after conjugation with herceptin, a humanized monoclonal antibody targeting the HER-2 receptor. Due to herceptin's therapeutic effect, the conjugate was simultaneously used for targeted imaging and therapy.[38b] Even deeper tissue pen-

etration would be possible if two-photon excitation was used for the AuNC-BSA.[39]

When combined with other contrast agents, the AuNC-BSA can be used for multimodal imaging.[38c–e] Yan and co-workers synthesized a multifunctional nanoprobe by *in situ* formation of Gd_2O_3 and AuNC within a BSA scaffold, and subsequent conjugation of tumour-targeting iRGD peptide. The nanoprobe exhibited multimodal imaging capability, i.e., NIR fluorescence imaging and magnetic resonance imaging (MRI).[38c] As shown in Figure 7, the AuNC/Gd_2O_3-BSA probe was successfully

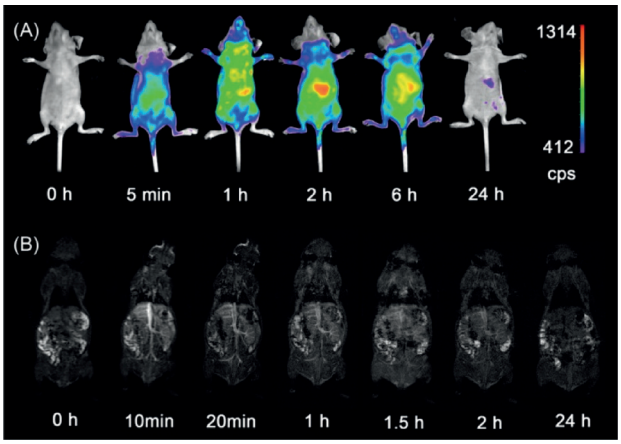

Figure 7. Multifunctional nanoprobe of AuNC/Gd_2O_3-BSA for NIR fluorescence (A) and MRI (B) imaging *in vivo*. Reprinted with permission from Ref. [38c]; copyright 2013 American Chemical Society.

used for blood pool imaging *in vivo*. When further conjugated with iRGD, the probe targeted imaging of U87-MG tumour-bearing mice *in vivo*.[38c] When the AuNC-BSA was conjugated onto an iron oxide magnetic NP, the conjugate could produce singlet oxygen ($^1O_2$), which in turn, triggered the formation of green fluorescent endoperoxide. Thus, the probe with $^1O_2$-sensitized fluorescence, and NIR and MRI triple imaging modality was obtained and used for live cell imaging.[38d]

Due to their high atomic number, gold atoms exhibit strong X-ray attenuation characteristics. Based on this, recent studies demonstrated that AuNC-BSA could be used for X-ray imaging, such as hard X-ray-induced optical luminescence and X-ray computed tomography (CT).[38f–h,j] Zhang and co-workers showed that AuNC-BSA possessed decent fluorescent and strong X-ray attenuation properties, which was then successfully used for fluorescent and CT dual-modality imaging.[38j] Inspired by these reports, Cai's group synthesized hybrid AuNC/Gd(III)-BSA for targeted NIR/CT/MRI triple-modal tumour imaging *in vivo*.[38h] Such multimodal synergistic imaging would allow more complementary structural and functional imaging information, which is critical for targeted imaging, as well as for other biomedical research.[38h]

Note: most of the above-discussed detection methods and imaging protocols can be readily extended to other FMNCs, or AuNCs stabilized by other proteins (or peptides) (*vide infra*).

2.1.2 AgNCs

Synthetic protocols. Compared with AuNCs, the synthesis of AgNCs is more challenging, due to their intrinsically more active chemistry. For example, AgNCs are easily oxidized and the reduction of Ag^+ to Ag^0 is sensitive to light exposure, etc. Several recent reports, however, have shown that AgNC-BSA can be prepared by carefully controlling the synthetic parameters (Figure S1).[11a,16,40]

For example, Guo *et al.* developed an interesting dBSA-directed approach to prepare Ag_{34}NC-dBSA.[11a] As shown in Figure 8a, to fully liberate the thiols of Cys from the disulfide bonds, BSA was denatured by guanidine hydrochloride and then reduced by tris(2-carboxyethyl)phosphine (TCEP). After uptake of Ag^+ ions by

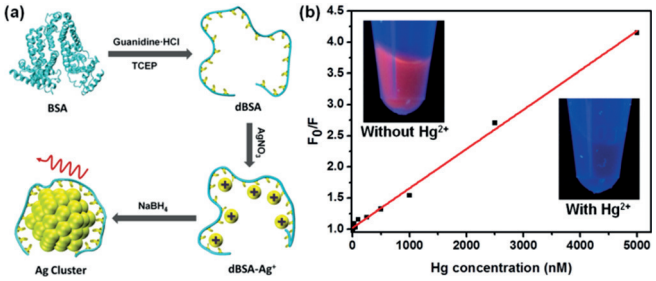

Figure 8. dBSA-directed approach to AgNCs. (a) Schematic of the dBSA-directed synthesis of fluorescent AgNCs; (b) the Stern-Volmer plot of fluorescence quenching of the Ag_{34}NC-dBSA by Hg^{2+}. Inset: the fluorescent images of the Ag_{34}NC-dBSA in the absence and presence of Hg^{2+} under UV light illumination. Reprinted with permission from Ref. [11a]; copyright 2011 American Chemical Society.

dBSA, they were reduced by $NaBH_4$ to form AgNC. Due to multiple coordination between the free Cys of dBSA and the surface-exposed Ag atoms, the formed Ag_{34}NC-dBSA exhibited excellent fluorescence at 637 nm and stability against a high salt solution. It could also be stored long-term. By modifying the synthetic approach to AuNC-BSA (Figure 4), several groups showed AgNC-BSA could also be obtained.[16,40] After the incubation of Ag^+ and BSA in the presence of NaOH, $NaBH_4$ was introduced to form the AgNC. Unlike the synthesis of AuNC-BSA, the addition of $NaBH_4$ is usually necessary. Both Ag_{15}NC and Ag_{13}NC were prepared, though almost the same synthetic parameters were adopted, indicating the sensitivity of AgNC formation to external environment.[40a,c] The reduction of Ag^+ in the presence of BSA by $NaBH_4$ in the dark produced Ag_8NC.[16]

Applications. Till now, most of the applications of AgNC-BSA have been focused on sensing. In Guo and

co-workers' study, they demonstrated for the first time that the Ag_{34}NC-dBSA could be used to detect Hg^{2+} with high sensitivity and selectivity (Figure 8b).[11a] Another independent study showed that the Ag_{15}NC-BSA could also sense Hg^{2+}.[40b] The determination of H_2O_2 was accomplished by quenching the fluorescence of Ag_{13}NC-BSA.[40c] Yang *et al.* reported a catalytic method to detect ascorbic acid. Ascorbic acid could reduce Ag^+ to form big plasmonic AgNPs when catalysed by the AgNC-BSA. By monitoring the plasmonic behaviour of the catalytically formed AgNPs, the colorimetric detection of ascorbic acid was realized.[40d] Similarly to AuNC-BSA, the AgNC-BSA also exhibited cathodic ECL behaviour, which could be further enhanced by dopamine. Thus, it has been used for dopamine detection.[40e]

2.1.3 Other Metal Nanoclusters

Studies demonstrated that BSA could also direct the formation of CuNCs and PtNCs, as well as doped and alloyed metal nanoclusters.[11b–d,41]

CuNCs. As shown in Figure S2, CuNCs can also be synthesized by using a BSA-directed approach.[11b,41] For example, blue-emitting CuNC was synthesized by reducing copper ions in the presence of BSA under alkaline conditions at an elevated temperature (55 °C) (Figure S2c).[11b] The CuNC emitted at 410 nm and was identified as Cu_5NC-BSA and Cu_{13}NC-BSA. Interestingly, the fluorescence of the CuNC-BSA could be quenched by Pb^{2+}, due to strong interaction between Pb^{2+} and BSA. Based on such quenching, levels as low as parts per million of Pb^{2+} were selectively detected.[11b] By exploring the peroxidase mimicking activity of the above CuNC-BSA, colorimetric detection of glucose was accomplished.[41a] The CuNC-BSA could also be used for the detection of kojic acid in food samples, as reported recently.[41b]

To overcome the limit of blue-emitting CuNCs in application for cellular imaging, Wang *et al.* developed a red-emitting CuNC-BSA with 625 nm emission (Figure S2b).[41c] It was synthesized by using hydrazine hydrate ($N_2H_4 \cdot 2H_2O$) as the reducing agent. The CuNC was successfully used for labelling and imaging CAL-27 cells. The CuNC was also used for selective oxidation of styrene to benzaldehyde.

PtNCs. Subnanometer-sized PtNC-BSA was also synthesized.[11c] The strong blue fluorescence at 404 nm of the PtNC-BSA could be quenched by hypochlorite. Thus, the sensing of hypochlorite with the PtNC was developed.

Doped AuNCs. When Ce^{4+} was included in the precursors, Ce-doped AuNC-BSA could be obtained.[11e] Chen *et al.* found that the doped AuNC exhibited dual emissions at 410 and 650 nm, respectively. Interestingly, the blue emission was sensitive to pH, while the red was insensitive (Figure 9a). They therefore employed the doped AuNC as ratiometric probes for monitoring cellular pH values (Figure 9b).

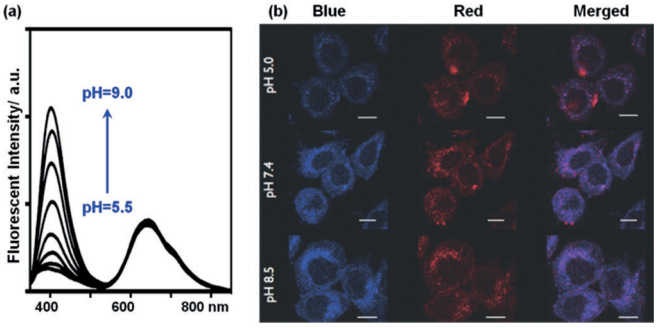

Figure 9. Ce-doped AuNC-BSA for ratiometrically sensing cellular pH. Reprinted with permission from Ref. [11e]; copyright 2014 Royal Society of Chemistry.

Alloyed NCs. Alloyed AuAgNC-BSA was prepared by Mohanty *et al.*[11d] As shown in Figures S3d and S3e, $Au_{38-x}Ag_x$NC-BSA has been obtained by both approaches. The composition of the alloyed clusters could be tailored by varying the ratio of the precursors. Inter-protein metal atom transfer was strongly implied to form such alloyed structures. Interestingly, the AuAgNC exhibited red-shifted emission, compared with both parent NCs.

2.2 Other Protein-directed Approaches

Wei *et al.* demonstrated that several other proteins besides BSA, such as lysozyme and cellular retinoic acid-binding protein II (CRABP-II), can be used to direct the formation of AuNCs.[10] Since then, numerous other proteins have been exploited to generate diverse FMNCs (Table S1). In this section, the synthesis of FMNCs with other proteins, rather than BSA, and their applications are briefly covered.

2.2.1 Lysozyme-directed Approach

The lysozyme-directed approach has been well summarized in a recent review, so only some selected examples are discussed here (Figure S4).[9e] Wei *et al.* reported the synthesis of AuNC-lysozyme (Figure S4a).[10] As shown in Figure 10, the formed AuNC-lysozyme emitted red fluorescence under UV irradiation. Moreover, the red emission could be selectively quenched by Hg^{2+}, primarily due to the specific metallophilic Hg^{2+}-Au^+ interaction. Thus, a method for Hg^{2+} detection was developed (Figure 10b). Other metal nanoclusters, such as AgNCs, CuNCs, PtNCs, and alloyed NCs, were also synthesized with lysozyme.[9e]

Since lysozyme itself is an enzyme, it is interesting to study its enzymatic activity after forming FMNCs. Chen *et al.* found that the bioactivity of lysozyme was indeed retained after forming AuNCs.[42] The AuNC-lysozyme bound to drug-resistant bacteria, as well as Gram-negative and positive bacteria. The AuNC-lysozyme also showed antimicrobial effects against the tested bacteria.

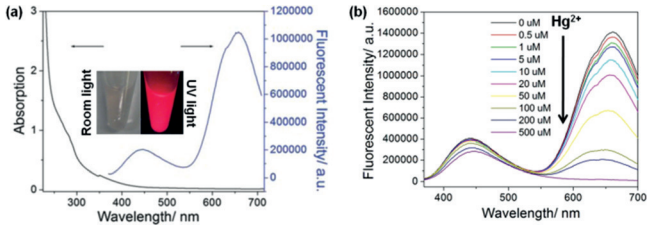

Figure 10. Lysozyme-directed approach to AuNCs. (a) UV-visible absorption (left) and fluorescent (right) spectra of the AuNC-lysozyme. Excitation wavelength = 360 nm. Inset: the AuNC-lysozyme under room light and UV irradiation. (b) Fluorescent spectra of the AuNC-lysozyme in the presence of different concentrations of Hg^{2+}. Reprinted with permission from Ref. [10]; copyright 2010 Royal Society of Chemistry.

Moreover, when carcinomic human alveolar basal epithelial A549 cells were treated by the AuNC-lysozyme, methylthiazolyldiphenyl-tetrazolium bromide (MTT), assays indicated excellent biocompatibility of the AuNC-lysozyme with the cells.[42]

Besides lysozyme, other hydrolyases, such as trypsin, chymotrypsin, pepsin, papain, ribonuclease-A, and DNase, have also been successfully employed to make FMNCs.[43] For example, following Xie's protocol, AuNC-trypsin was prepared. The AuNC-trypsin was then conjugated with folic acid for *in vivo* tumour imaging.[43a] Similarly, CuNC-trypsin was prepared.[43b] Interestingly, the CuNC-trypsin exhibited reversible fluorescent response to pH changes between pH 2.4 and pH 11.4. A hydrolyase may autolyse itself. By ingeniously making use of this property of pepsin, Kawasaki reported the pH-dependent synthesis of AuNCs-pepsin with different sizes and fluorescent emissions (Figure S5).[43d]

2.2.2 HSA-directed Approach

HSA was employed to prepare AuNCs and AgNCs. For example, AuNC-HSA was synthesized via a microwave-assisted method and used for NO_x sensing due to the quenching effect.[44] Unexpectedly, Chan *et al.* discovered that the AuNC-HSA exhibited unique and selective affinity toward *S. aureus* and methicillin-resistant *S. aureus*.[45] They further identified the peptide sequence responsible for the specific binding. The peptides' selective binding affinity was further confirmed by testing the interactions of the bacteria and the synthetic peptide-stabilized AuNC. In another study, Ag_9NC-HSA and Ag_{14}NC-HSA were prepared by Ghosh and co-workers.[46] They showed that the emission of the Ag_9NC could be reversibly switched off by Co^{2+} and switched on by Zn^{2+}. The fluorescence of the Ag_{14}NC, on the other hand, was specifically quenched by Hg^{2+} (Figure S6). The Ag_9NC-HSA and Ag_{14}NC-HSA were actually interconvertable.[47]

Other albumins, such as lactalbumin and ovalbumin, have also been utilized to fabricate FMNCs.[48] In practical synthesis, chicken egg white, which mainly consists of ovalbumin (54%), ovotransferrin (12%), ovomucoid (11%), and lysozyme (3.4%), was usually used to form FMNCs. Since ovalbumin is a glycoprotein, the glycan of ovalbumin can be recognized and bound by lectins, such as concanavalin A (Con A), even after the formation of AuNCs.[48c] Even eggshell membrane has been used to generate fluorescent AuNCs.[49]

2.2.3 Other Protein-directed Approaches

Till now, numerous other proteins (such as ferritin, transferritin, horseradish peroxidase (HRP), hemoglobin, insulin, etc.) have been investigated to form FMNCs, as summarized in Table S1.[15,50]

Sun *et al.* were able to form paired AuNCs within the cage of horse spleen ferritin.[50a] Compared with single AuNC, the paired AuNCs exhibited not only enhanced, but also red-shifted, fluorescent emission. The paired AuNCs-ferritin could be taken up by the kidney for *in vivo* imaging, which was mediated by the ferritin receptors being present in certain cells of the kidney. Wang *et al.* showed that the fluorescence of AuNC-transferrin was quenched by graphene oxide, but could be recovered after cell uptake.[50b] Thus, a turn-on cellular and small animal imaging protocol was developed. Chaudhari *et al.* performed a careful mechanism study of AuNC evolution using lactoferrin as a model protein (Figure S7).[15] Clearly, the evolution from a small-sized AuNC to a large-sized one, as well as the regeneration of free lactoferrin and inter-protein Au atom transfer, were demonstrated, suggesting a possible mechanism of: protein $+HAuCl_4 \rightarrow$ [Au(I)-protein] (low pH)$\rightarrow$small AuNC-protein (low to neutral pH)$\rightarrow$large AuNC-protein (high pH).

The formation of FMNCs *in situ* within cell matrices and mice was also reported, suggesting great promise of *in cellulo* (*in vivo*) chemistry for a plethora of applications, such as in bioimaging, biolabelling, and synthetic biology.[51]

2.2.4 Effects of Protein Characteristics

Several studies were devoted to understanding the effects of protein characteristics on the formation of FMNCs.[13,48a,52] Some conclusions could be summarized, though a relatively small library of proteins were studied. First, the size, isoelectric point, flexibility (rigidity), and 3-dimensional structure of the protein, as well as its amino acid content, can affect the formation of FMNCs.[52] Second, the rigid structure and high Arg content may lead to lower stability of the formed AuNC (such as AuNC-lysozyme vs AuNC-BSA).[48a] Third, though Tyr/Trp residues are mainly reducing amino acids, they must be balanced by the amine-containing residues. A protein with too many Tyr/Trp residues compared with amine-containing residues may not be able to form

FMNCs.[13] Fourth, blue-shifted emission would be observed if a protein contained low Cys content (< 18 Cys/protein).[13] Fifth, large-sized proteins would endow the FMNCs with high photo, thermal, chemical, and long-term stability.[13]

3 Peptide-directed Approaches

Both naturally occurring and designed peptides have been exploited to produce FMNCs with high quality. Besides the common attributes provided by the protein-directed approach, the peptide-directed approach has several unique advantages.[53] First, peptide is easier to synthesize. Second, it can be assembled into designed structures. Third, certain selected peptides have specific recognition capability and binding affinity toward their targets. Fourth, with defined and distinctive sequences, the directing roles of the amino acids of a peptide in forming FMNCs may be elucidated. Further, it is even possible to rationally design peptides with required properties to controllably produce new FMNCs with enhanced functionalities. In this section, the use of natural peptides (mainly GSH), as well as designed peptides, to prepare FMNCs are discussed.

3.1 GSH-directed Approach

GSH, having the sequence of γ-Glu-Gly-Cys, is the most studied natural peptide for the preparation of FMNCs. It has been used as a ligand for metal NC synthesis (especially for AuNCs and AgNCs) since the early stages of NC studies.[54] Their photoluminescent properties have also been extensively investigated.[6c,55] Here, both the synthetic protocols, as well as the applications of GSH-stabilized FMNCs, are discussed (Table S2).

3.1.1 AuNCs

Synthetic protocols. Most of the FMNCs stabilized by GSH were synthesized by adopting the protocol developed by Schaaff and co-workers.[54] For AuNC-GSH, the mixing of $HAuCl_4$ with GSH formed the Au^+-GSH oligomer. The further addition of $NaBH_4$ then reduced Au^+ to Au^0 and induced the subsequent assembly into AuNCs (Figure 11).[54b] Since the obtained product was a mixture of AuNCs with different sizes, separation (such as high resolution polyacrylamide gel electrophoresis (PAGE)) was usually employed to isolate pure AuNC components.[55] For example, as many as nine kinds of AuNCs were identified using PAGE combined with mass spectroscopy.[55] However, the QYs of initially synthesized AuNCs were not very high. Later, highly fluorescent metal NCs stabilized by GSH were prepared by improved synthesis.

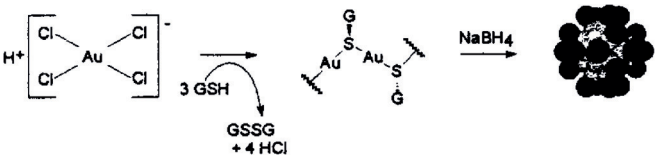

Figure 11. GSH-directed approach to AuNCs. First, $HAuCl_4$ was reduced with GSH to form the Au^+-GSH oligomer; the oligomer was then further reduced by $NaBH_4$ to generate the AuNCs. Reprinted with permission from Ref. [54b]; copyright 2000 American Chemical Society.

It was discovered that Au^+-thiolate complexes exhibited interesting and strong aggregation-induced emission (AIE).[56] By *in situ* formation of such Au^+-thiolate complexes onto a reduced Au^0 core, highly fluorescent AuNC-GSH was obtained (Figure 12 and Figure S8).

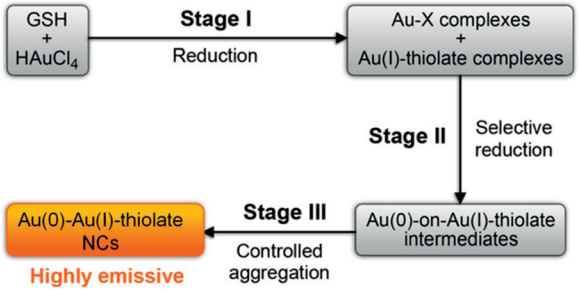

Figure 12. GSH-directed approach to AuNCs via controlled formation of Au(I)-thiolate onto Au^0 core. Reprinted with permission from Ref. [56]; copyright 2012 American Chemical Society.

Compared with AuNC-GSH synthesized by the conventional protocol (Figure 11), the highly fluorescent emission of AuNC by the method in Figure 12 was mainly attributed to the presence of oligomeric Au^+-thiolate complexes. The proposed new method was scalable and could be extended to other thiolate ligands.[56] Large quantities of discrete AuNCs-GSH could be obtained by a pH-controlled CO reduction approach or a two-phase approach.[57] However, the fluorescent properties of these AuNCs remain to be investigated.

Applications. Similarly to protein-stabilized AuNCs, the AuNC-GSH has also been used for biosensing, and cellular and *in vivo* imaging, etc. For example, selective Cu^{2+} detection was reported, based on its quenching effect on the fluorescence of AuNCs.[58]

Recently, Chen *et al.* developed a ratiometric probe for living cell imaging of highly reactive oxygen species (hROS).[59] The dual emission probe was made by assembling an oligoarginine peptide-modified AuNC-GSH onto dye-loaded silica NPs (SiNPs). As shown in Figure 13, the SiNPs were insensitive to hROS due to silica shell protection. However, the fluorescence of AuNC-GSH would be quenched by hROS. Due to the oligoarginine peptide's

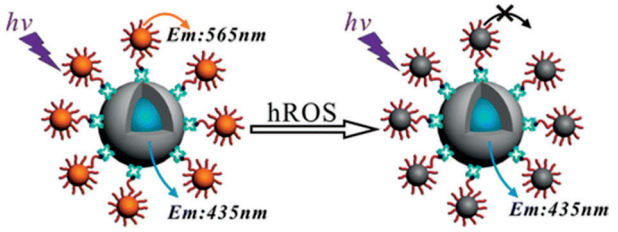

Figure 13. hROS detection with a dual emission probe assembled from dye-loaded SiNP and AuNC-GSH. Reprinted with permission from Ref. [59]; copyright 2013 American Chemical Society.

cell penetration capability, the probe could be readily taken up by cells and used for rapidly sensing hROS in living cells with high selectivity.[59]

Due to its NIR fluorescence and X-ray attenuation capability, AuNC-GSH has been exploited for optical, MRI, and dual modal imaging. Compared with NIR dye (such as IRDye 800CW) and AuNC-BSA, AuNC-GSH has exhibited several distinguished features for *in vivo* imaging.[60] First, the capping GSH is resistant to enzymatic digestion, rendering the AuNC-GSH with good physiological stability.[61] Second, GSH can minimize serum protein adsorption.[62] Third, the AuNC-GSH can be efficiently cleared via kidney filtration and renal excretion, due to its ultrasmall size and surface chemistry. It was also found that AuNC-GSH can escape the reticuloendothelial system.[61] Fourth, despite its small size, AuNC-GSH still exhibits enhanced and extended tumour accumulation and fast normal tissue clearance, which is attributed to the enhanced permeability and retention (EPR) effect.[60a,63] With these distinct advantages, AuNC-GSH could be used for both diagnostics and therapy.[60–64]

3.1.2 AgNCs

Numerous studies have also been focused on the synthesis and applications of AgNC-GSH. Recently, an effective cyclic reduction-decomposition synthetic protocol combined with etching was developed to produce high fluorescent AgNC-GSH with tuneable emissions.[65] As shown in Figure 14, the initially obtained AgNC intermediates in Stage I were further etched to get highly luminescent AgNCs. AgNCs-GSH with both green (Ag_9NC) and red (Ag_{16}NC) emissions were obtained. A following study showed that other AgNCs, such as Ag_{15}NC and Ag_{31}NC, were also made.[66] The AgNC-GSH possessed excellent antimicrobial properties.[65] Moreover, Cys detection was achieved with the AgNC-GSH because Cys could penetrate the GSH capping layer and decompose the AgNC to nonfluorescent thiolate-Ag^+ complexes.[8b]

Using large AgNPs as the starting materials, AgNC-GSH was prepared by GSH-mediated etching at 65 °C. By controlling the etching time, AgNCs with blue-green, yellow, and red emissions were produced.[67] Among the three AgNCs, the yellow emitting one had a QY over

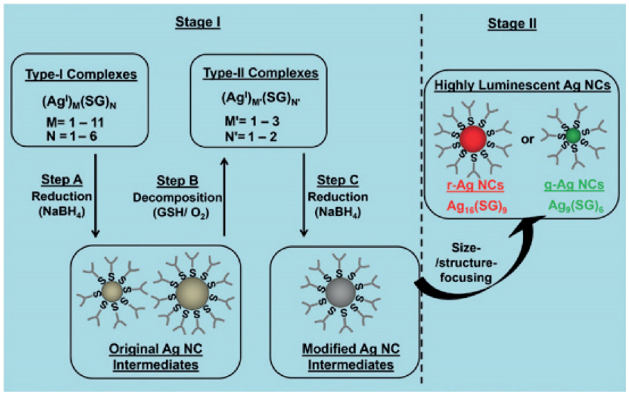

Figure 14. Cyclic reduction-decomposition synthetic protocol, combined with etching for AgNC-GSH. Reprinted with permission from Ref. [65]; copyright 2013 Nature Publishing Group.

60 % and was used for cancer cell imaging. The AgNCs-GSH with different emissions could also be made by tuning the ratios of $AgNO_3$ to GSH and the reaction temperature.[68] When Ag^+ was preloaded within polyacrylamide gel, sunlight could induce the *in situ* formation of AgNC.[69]

3.1.3 Other Metal Nanoclusters

By etching PtNPs with GSH, yellow emitting PtNC-GSH was prepared by Le Guevel and co-workers.[70]

When the mixture of GSH, $HAuCl_4$, and $AgNO_3$ was exposed to sunlight, a unique Au-Ag hybrid NC was obtained.[71] It suggested that giant hybrid NC had an Au(I) core and an Ag_2 and Ag_3 shell. The NC was used for selective detection of Hg^{2+}.

3.2 Designed Peptide-directed Approach

Many rationally designed peptides have also been used to prepare FMNCs (Table S3). Previous studies have shown that peptides as short as a single amino acid can be used to form FMNCs.[72a] Dipeptide, tripeptide, and longer peptides have been successfully designed to generate FMNCs.[72b] In this section, we first try to summarize certain rules that may guide the design of peptide for synthesis of FMNCs. Then, the representative synthetic protocols and selected applications are discussed.

3.2.1 General Design Rules

As shown in Table S3, many designed peptides have been exploited to make FMNCs. Based on these studies, empirical rules guiding the design of peptide sequences for the formation of FMNCs are summarized here. Notably, FMNCs can be formed via reduction of metal ion precursors, either with the amino acids in a peptide or using external reducing agents (*vide infra*).

Previous studies have demonstrated that Cys and Tyr are essential to form FMNCs (especially AuNCs) if no external reducing agent is added.[8e,10,73] It has also been shown that Cys and Tyr cannot be replaced by Met and Trp, respectively.[73] As shown in Figure 15a, to direct the formation of FMNCs, the peptide should consist of three parts: (a) the directing sequence that is responsible for the formation of FMNCs; (b) the recognition (functional) sequence that is for specific target binding (or other functions); and (c) the linker sequence that is used to connect directing and recognition parts together and to minimize the potential cross-talk (interference) of the two parts. In the illustrative sequence 1 shown in Figure 15a, the CCY was for $Cu_{14}NC$ formation.[74] More specifically, the CC was for stabilizing the $Cu_{14}NC$, while the Y was for the reduction of Cu ions under an alkaline pH. The PKKKRKVG, a nuclear localization sequence, was for cell nuclei targeting. The GG was used to connect the other two parts into a single peptide. Such a design can be readily extended to other FMNCs, such as AuNCs and AgNCs. Sometimes, a linker may not be essential. In the sequence 2 shown in Figure 15a, the CCY sequence could be directly attached onto the RGRKKRRQRRR sequence, the TAT sequence for cell penetration. The designed peptide can be used to form AuNCs and AgNCs.[8f,75] When the reducing amino acid Y is absent in a designed peptide, an external reducing agent, such as $NaBH_4$, is usually needed to promote the reduction of metal ion precursors to FMNCs. The studies suggested the location of C and/or Y in a peptide also affected the FMNCs formation.[73] However, no exact relationship has been elucidated yet. The final size of FMNCs may be controlled by the 3-dimensional structure of the designed peptide, as illustrated by a recent report.[76]

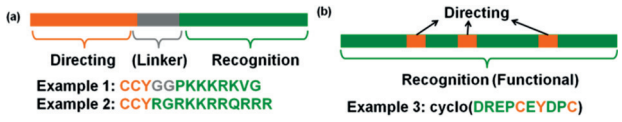

Figure 15. Possible rules for designing peptides, which can direct the formation of FMNCs. (a) A peptide may consist of three parts: the directing (synthetic) part, the recognition (functional) part, and the linker part that connects the directing and recognition parts. Sometimes, a linker may not be necessary. (b) The directing amino acids may be incorporated into a recognition (functional) peptide.

As shown in Figure 15b, the directing amino acids may be incorporated into a recognition peptide. For example, when three amino acids of the cyclodecapeptide for Gd^{3+} binding were replaced by two C and one Y, the designed peptide was able to form dual functional Gd^{3+}-AuNC (Example 3 in Figure 15b).[77] However, such incorporation may disturb functions of the recognition sequence. Thus, more careful design is needed.

It was also shown that the presence of hydrophobic amino acids may improve the stability of formed FMNCs.[78] Söptei *et al.* suggested the existence of a critical ratio of Cys to metal ion precursors to form FMNCs. Only above the ratio, would FMNCs form. Otherwise, larger NPs may be produced.[73]

Following the rules summarized above, one should be able to prepare FMNCs with desired functions by rationally designing the peptide sequence. Such design rules should be applicable to other nanomaterials. They may also be extended to other biomolecules, rather than peptides, such as nucleic acids and peptide-nucleic acid chimeras. Despite this, great efforts are needed to reveal more factors which control the formation of FMNCs with peptides.

3.2.2 Synthetic Protocols and Applications

As shown in Figure S9 and discussed above, FMNCs can be synthesized via the reduction of metal ion precursors, either with the amino acids (mainly Tyr) in a peptide or using external reducing agents (such as $NaBH_4$).

For example, $Ag_{28}NC$ and $Au_{25}NC$ were obtained with the peptide CCYRGRKKRRQRRR at an alkaline pH (pH = 12).[8f,75] It was shown that synthetic pH plays an important role in the final size of FMNCs. Cui *et al.* prepared Ag_5NC, Ag_6NC, and Ag_7NC using the same peptide for $Ag_{28}NC$, but at lower pH (pH = 9).[8f] For each FMNC, the synthetic parameters should be optimized. For example, to get $Cu_{14}NC$, an incubation temperature as high as 80 °C was needed.[74]

For the peptide without Tyr residues, usually $NaBH_4$ is added for the reduction. As shown in Figure S9c, NaOH may be also introduced, depending on the peptides used. Wen *et al.* demonstrated the use of 3-mercaptopropionic acid as an auxiliary ligand which enhanced the fluorescence of the formed AuNCs due to better surface passivation.[79]

Many interesting applications of peptide-stabilized FMNCs are summarized in Table S3. Here, a few selected examples are covered. In Wen and co-workers' study, the peptides consisting of CC and enzyme substrate sequences were used to form AuNCs.[79] After the enzymatic treatment of the peptides stabilized AuNCs, their fluorescence decreased, which was probably due to the disturbance of the interactions between the peptide and AuNC core. For example, when the peptide with CCLRRASLG sequence was used to form AuNC, the obtained AuNC could detect the activity of protein kinase A by monitoring the fluorescence decrease. This was a general sensing platform. When other enzyme substrates were embedded within the FMNCs directing peptides, the activity of the corresponding enzymes could be determined. Moreover, the enzyme inhibitors could also be screened with such FMNCs as the fluorescent probes.[79]

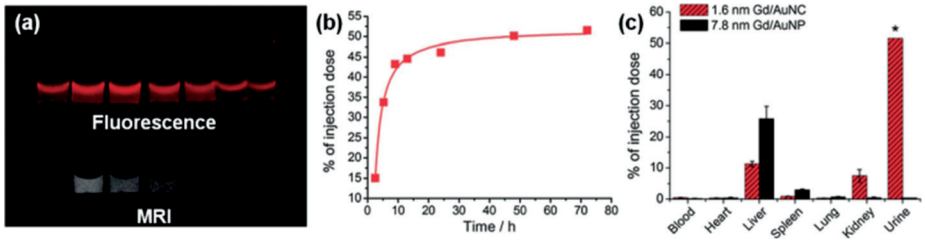

Figure 16. Renal clearance and biodistribution of Gd^{3+}-AuNC. (a) Fluorescence and MR images of Gd-AuNC in urine collected at different time after injection; (b) gold contents in the urine samples measured by ICP-AES; (c) biodistribution of Gd^{3+}-AuNC and Gd^{3+}-AuNP after 24 h injection. Reprinted with permission from Ref. [77]; copyright 2013 Royal Society of Chemistry.

Liang *et al.* developed a Gd^{3+}-functionalized AuNC for fluorescence and MRI dual model imaging.[77] As discussed in Figure 15b, the cyclodecapeptide was used to form the Gd^{3+}-AuNC. Both cellular and *in vivo* animal imaging was accomplished with the dual function probe. More interesting, due to the ultrasmall size, the probes were noticeably excreted from the body through renal clearance after 24 h injection (Figure 16). As a comparison, the large probe with 7.8 nm AuNP could not be cleared.

4 Summary and Outlook

This review paper summarizes the recent progress in protein- and peptide-directed approaches for a myriad of FMNCs. The synthetic protocols, formation mechanisms, and key applications are discussed (Tables S1–S3). Based on the discussions above, a few key conclusions could be drawn as follows. First, biomolecules, especially proteins and peptides, can direct the formation of functional nanomaterials with rationally designed properties for broad applications.[9e] Second, certain key amino acid residues, such as Cys and Tyr, play critical roles in directing the formation of FMNCs. Third, the 3-dimensional structures and the unique microenvironments of proteins and peptides also greatly affect FMNC formation. Fourth, the synthesis of multifunctional FMNCs, as well as other nanomaterials, is feasible when both directing and functional sequences are carefully designed and combined.

Though substantial progress has been achieved in the field, several challenges for further advancement remain to be addressed. First, the current understanding of the relationship of amino acid content, peptide length, and peptide structure with FMNC properties (such as fluorescent emission wavelength and QY) is still very limited. Advanced characterization techniques, combined with computation, would address this challenge.[80] Second, it is even more challenging to *de novo* design a protein (or assembled peptides) to direct the formation of FMNCs with tuneable properties.[81] Third, the structural information of the FMNCs is greatly needed. In contrast to thiolate ligand-stabilized MNCs, no crystal structures of protein-stabilized (or peptide-stabilized) FMNCs have been reported till now, which would provide us with deep insights if obtained.[82] Also, improved synthetic methods are needed to get large quantities of atomically precise FMNCs with enhanced performance. Finally, most of the applications are focused on biosensing and bioimaging; other applications should also be explored in the future.

In a nutshell, high-performance FMNCs with defined structures and desired properties in protein and peptide (as well as other biomolecules) templates are expected to be *de novo* designed, synthesized, and applied in various areas in the future.

Acknowledgements

We would like to thank the National Natural Science Foundation of China (no. 21405081), the Natural Science Foundation of Jiangsu Province (no. BK20130561), the 973 Program (no. 2015CB659400), the 985 Program of Nanjing University, the Priority Academic Program Development of Jiangsu Higher Education Institutions (PAPD), the Fundamental Research Funds for the Central Universities (no. 20620140627), the Open Funds of the State Key Laboratory of Electroanalytical Chemistry (SKLEAC201501), the Shuangchuang Program of Jiangsu Province, the Six Talents Summit Program of Jiangsu Province, and the Thousand Talents Program for Young Researchers for financial support.

References

[1] a) M. C. Daniel, D. Astruc, *Chem. Rev.* **2004**, *104*, 293–346; b) H. Wei, B. L. Li, Y. Du, S. J. Dong, E. Wang, *Chem. Mater.* **2007**, *19*, 2987–2993; c) H. Wei, J. Li, Y. L. Wang, E. K. Wang, *Nanotechnology* **2007**, *18*, 175610; d) L. L. Sun, Y. H. Song, L. Wang, C. L. Guo, Y. J. Sun, Z. L. Liu, Z. Li, *J. Phys. Chem. C* **2008**, *112*, 1415–1422; e) H. Wei, E. K. Wang, *Nanotechnology* **2007**, *18*, 295603; f) F. G. Xu, K. Cui, Y. J. Sun, C. L. Guo, Z. L. Liu, Y. Zhang, Y. Shi, Z. Li, *Talanta* **2010**, *82*, 1845–1852; g) C. L. Guo, Y. H. Song, L. Wang, L. L. Sun, Y. J. Sun, C. Y. Peng, Z. L. Liu, T. Yang, Z. Li, *J. Phys. Chem. B* **2008**, *112*, 1022–1027; h) Y. J. Sun, L. Wang, L. L. Sun, C. L. Guo, T. Yang, Z. L. Liu, F. G. Xu, Z.

Li, *J. Chem. Phys.* **2008**, *128*, 074704; i) C. L. Guo, Z. L. Liu, F. G. Xu, L. L. Sun, Y. J. Sun, T. Yang, Z. Li, *J. Phys. Chem. B* **2009**, *113*, 6068–6073; j) X. H. Liu, L. X. Zhang, Y. L. Wang, C. L. Guo, E. K. Wang, *Cryst. Growth Des.* **2008**, *8*, 759–762; k) C. L. Guo, G. P. Li, Z. L. Liu, L. L. Sun, Y. J. Sun, F. G. Xu, Y. Zhang, T. Yang, Z. Li, *ChemPhysChem* **2009**, *10*, 1624–1629; l) Z. Zhen, W. Tang, C. Guo, H. Chen, X. Lin, G. Liu, B. Fei, X. Chen, B. Xu, J. Xie, *ACS Nano* **2013**, *7*, 6988–6996; m) S. Mura, G. Greppi, P. Innocenzi, M. Piccinini, C. Figus, M. L. Marongiu, C. L. Guo, J. Irudayaraj, *J. Raman Spectrosc.* **2013**, *44*, 35–40.

[2] a) N. L. Rosi, C. A. Mirkin, *Chem. Rev.* **2005**, *105*, 1547–1562; b) H. Wei, B. L. Li, J. Li, E. K. Wang, S. J. Dong, *Chem. Commun.* **2007**, 3735–3737; c) H. Wei, B. L. Li, J. Li, S. J. Dong, E. K. Wang, *Nanotechnology* **2008**, *19*, 095501; d) Z. Z. Lv, H. Wei, B. L. Li, E. K. Wang, *Analyst* **2009**, *134*, 1647–1651; e) H. Wei, C. G. Chen, B. Y. Han, E. K. Wang, *Anal. Chem.* **2008**, *80*, 7051–7055; f) Y. Wang, H. Wei, B. Li, W. Ren, S. Guo, S. Dong, E. Wang, *Chem. Commun.* **2007**, 5220–5222; g) B. L. Li, Y. L. Wang, H. Wei, S. J. Dong, *Biosens. Bioelectron.* **2008**, *23*, 965–970; h) H. Wang, H. Sun, H. Wei, P. Xi, S. Nie, Q. Ren, *J. Nanopart. Res.* **2014**, *16*, 2621; i) S. Zhang, Y. Ding, H. Wei, *Molecules*, **2014**, *19*, 11933–11987; j) L. Zhang, H. Wei, J. Li, T. Li, D. Li, Y. Li, E. Wang, *Biosens. Bioelectron.* **2010**, *25*, 1897–1901.

[3] D. Jariwala, V. K. Sangwan, L. J. Lauhon, T. J. Marks, M. C. Hersam, *Chem. Soc. Rev.* **2013**, *42*, 2824–2860.

[4] a) M. Bruchez, M. Moronne, P. Gin, S. Weiss, A. P. Alivisatos, *Science* **1998**, *281*, 2013–2016; b) W. C. W. Chan, S. M. Nie, *Science* **1998**, *281*, 2016–2018; c) X. Michalet, F. F. Pinaud, L. A. Bentolila, J. M. Tsay, S. Doose, J. J. Li, G. Sundaresan, A. M. Wu, S. S. Gambhir, S. Weiss, *Science* **2005**, *307*, 538–544; d) J. Yao, M. Yang, Y. X. Duan, *Chem. Rev.* **2014**, *114*, 6130–6178.

[5] K. E. Sapsford, W. R. Algar, L. Berti, K. B. Gemmill, B. J. Casey, E. Oh, M. H. Stewart, I. L. Medintz, *Chem. Rev.* **2013**, *113*, 1904–2074.

[6] a) L. A. Peyser, A. E. Vinson, A. P. Bartko, R. M. Dickson, *Science* **2001**, *291*, 103–106; b) T. Huang, R. W. Murray, *J. Phys. Chem. B* **2001**, *105*, 12498–12502; c) S. Link, A. Beeby, S. FitzGerald, M. A. El-Sayed, T. G. Schaaff, R. L. Whetten, *J. Phys. Chem. B* **2002**, *106*, 3410–3415; d) J. Zheng, R. M. Dickson, *J. Am. Chem. Soc.* **2002**, *124*, 13982–13983; e) J. T. Petty, J. Zheng, N. V. Hud, R. M. Dickson, *J. Am. Chem. Soc.* **2004**, *126*, 5207–5212; f) J. Zheng, P. R. Nicovich, R. M. Dickson, *Annu. Rev. Phys. Chem.* **2007**, *58*, 409–431; g) L. Shang, S. J. Dong, G. U. Nienhaus, *Nano Today* **2011**, *6*, 401–418; h) Q. F. Yang, J. Y. Liu, H. P. Chen, X. X. Wang, Q. M. Huang, Z. Shan, *Prog. Chem.* **2011**, *23*, 880–892; i) Y. C. Shiang, C. C. Huang, W. Y. Chen, P. C. Chen, H. T. Chang, *J. Mater. Chem.* **2012**, *22*, 12972–12982; j) L. B. Zhang, E. K. Wang, *Nano Today* **2014**, *9*, 132–157; k) J. Sun, Y. D. Jin, *J. Mater. Chem. C* **2014**, *2*, 8000–8011; l) Z. Luo, K. Zheng, J. Xie, *Chem. Commun.* **2014**, *50*, 5143–5155; m) J. Li, J.-J. Zhu, K. Xu, *TrAC Trends Anal. Chem.* **2014**, *58*, 90–98; n) S. Choi, R. M. Dickson, J. H. Yu, *Chem. Soc. Rev.* **2012**, *41*, 1867–1891; o) Y. Z. Lu, W. Chen, *Chem. Soc. Rev.* **2012**, *41*, 3594–3623; p) W. W. Guo, J. P. Yuan, Q. Z. Dong, E. K. Wang, *J. Am. Chem. Soc.* **2010**, *132*, 932–934; q) W. Wei, Y. Lu, W. Chen, S. Chen, *J. Am. Chem. Soc.* **2011**, *133*, 2060–2063; r) T. Vosch, Y. Antoku, J. C. Hsiang, C. I. Richards, J. I. Gonzalez, R. M. Dickson, *Proc. Natl. Acad. Sci. U.S.A.* **2007**, *104*, 12616–12621; s) P. Crespo, R. Litran, T. C. Rojas, M. Multigner, J. M. de la Fuente, J. C. Sanchez-Lopez, M. A. Garcia, A. Hernando, S. Penades, A. Fernandez, *Phys. Rev. Lett.* **2004**, *93*, 087204; t) A. Venzo, S. Antonello, J. A. Gascon, I. Guryanov, R. D. Leapman, N. V. Perera, A. Sousa, M. Zamuner, A. Zanella, F. Maran, *Anal. Chem.* **2011**, *83*, 6355–6362; u) R. S. McCoy, S. Choi, G. Collins, B. J. Ackerson, C. J. Ackerson, *ACS Nano* **2013**, *7*, 2610–2616.

[7] a) X. H. Gao, L. L. Yang, J. A. Petros, F. F. Marshal, J. W. Simons, S. M. Nie, *Curr. Opin. Biotechnol.* **2005**, *16*, 63–72; b) J. L. Yan, M. C. Estevez, J. E. Smith, K. M. Wang, X. X. He, L. Wang, W. H. Tan, *Nano Today* **2007**, *2*, 44–50; c) J. Zhou, Z. Liu, F. Y. Li, *Chem. Soc. Rev.* **2012**, *41*, 1323–1349; d) C. Guo, B. Book-Newell, J. Irudayaraj, *Chem. Commun.* **2011**, *47*, 12658–12660.

[8] a) X. K. Wan, Z. W. Lin, Q. M. Wang, *J. Am. Chem. Soc.* **2012**, *134*, 14750–14752; b) X. Yuan, Y. Q. Tay, X. Y. Dou, Z. T. Luo, D. T. Leong, J. P. Xie, *Anal. Chem.* **2013**, *85*, 1913–1919; c) L. Shang, N. Azadfar, F. Stockmar, W. Send, V. Trouillet, M. Bruns, D. Gerthsen, G. U. Nienhaus, *Small* **2011**, *7*, 2614–2620; d) H. W. Duan, S. M. Nie, *J. Am. Chem. Soc.* **2007**, *129*, 2412–2413; e) J. P. Xie, Y. G. Zheng, J. Y. Ying, *J. Am. Chem. Soc.* **2009**, *131*, 888–889; f) Y. Cui, Y. Wang, R. Liu, Z. Sun, Y. Wei, Y. Zhao, X. Gao, *ACS Nano* **2011**, *5*, 8684–8689; g) R. H. Terrill, T. A. Postlethwaite, C. H. Chen, C. D. Poon, A. Terzis, A. D. Chen, J. E. Hutchison, M. R. Clark, G. Wignall, J. D. Londono, R. Superfine, M. Falvo, C. S. Johnson, E. T. Samulski, R. W. Murray, *J. Am. Chem. Soc.* **1995**, *117*, 12537–12548; h) A. C. Templeton, M. P. Wuelfing, R. W. Murray, *Acc. Chem. Res.* **2000**, *33*, 27–36; i) J. F. Parker, C. A. Fields-Zinna, R. W. Murray, *Acc. Chem. Res.* **2010**, *43*, 1289–1296; j) P. D. Jadzinsky, G. Calero, C. J. Ackerson, D. A. Bushnell, R. D. Kornberg, *Science* **2007**, *318*, 430–433; k) L. Fabris, S. Antonello, L. Armelao, R. L. Donkers, F. Polo, C. Toniolo, F. Maran, *J. Am. Chem. Soc.* **2006**, *128*, 326–336; l) A. H. Holm, M. Ceccato, R. L. Donkers, L. Fabris, G. Pace, F. Maran, *Langmuir* **2006**, *22*, 10584–10589; m) S. Antonello, N. V. Perera, M. Ruzzi, J. A. Gascon, F. Maran, *J. Am. Chem. Soc.* **2013**, *135*, 15585–15594.

[9] a) M. B. Dickerson, K. H. Sandhage, R. R. Naik, *Chem. Rev.* **2008**, *108*, 4935–4978; b) H. Wei, Z. D. Wang, J. O. Zhang, S. House, Y. G. Gao, L. M. Yang, H. Robinson, L. H. Tan, H. Xing, C. J. Hou, I. M. Robertson, J. M. Zuo, Y. Lu, *Nat. Nanotechnol.* **2011**, *6*, 93–97; c) H. Wei, Y. Lu, *Chem. Asian J.* **2012**, *7*, 680–683; d) H. Wei, S. House, J. J. X. Wu, J. Zhang, Z. D. Wang, Y. He, E. J. Gao, Y. G. Gao, H. Robinson, W. Li, J. M. Zuo, I. M. Robertson, Y. Lu, *Nano Res.* **2013**, *6*, 627–634; e) Y. B. Ding, L. L. Shi, H. Wei, *J. Mater. Chem. B* **2014**, *2*, 8268–8291; f) S. R. Whaley, D. S. English, E. L. Hu, P. F. Barbara, A. M. Belcher, *Nature* **2000**, *405*, 665–668; g) R. R. Naik, S. J. Stringer, G. Agarwal, S. E. Jones, M. O. Stone, *Nat. Mater.* **2002**, *1*, 169–172.

[10] H. Wei, Z. D. Wang, L. M. Yang, S. L. Tian, C. J. Hou, Y. Lu, *Analyst* **2010**, *135*, 1406–1410.

[11] a) C. L. Guo, J. Irudayaraj, *Anal. Chem.* **2011**, *83*, 2883–2889; b) N. Goswami, A. Giri, M. S. Bootharaju, P. L. Xavier, T. Pradeep, S. K. Pal, *Anal. Chem.* **2011**, *83*, 9676–9680; c) X. D. Xia, Y. Zhang, J. X. Wang, *RSC Adv.* **2014**, *4*, 25365–25368; d) J. S. Mohanty, P. L. Xavier, K. Chaudhari, M. S. Bootharaju, N. Goswami, S. K. Pal, T. Pradeep, *Nanoscale* **2012**, *4*, 4255–4262; e) Y.-N. Chen, P.-C. Chen, C.-W. Wang, Y.-S. Lin, C.-M. Ou, L.-C. Ho, H.-T. Chang, *Chem. Commun.* **2014**, *50*, 8571–8574.

[12] a) T. Das, P. Ghosh, M. S. Shanavas, A. Maity, S. Mondal, P. Purkayastha, *Nanoscale* **2012**, *4*, 6018–6024; b) G. Guan, S.-Y. Zhang, Y. Cai, S. Liu, M. S. Bharathi, M. Low, Y. Yu, J. Xie, Y. Zheng, Y.-W. Zhang, M.-Y. Han, *Chem. Commun.* **2014**, *50*, 5703–5705.

[13] Y. Xu, J. Sherwood, Y. Qin, D. Crowley, M. Bonizzoni, Y. Bao, *Nanoscale* **2014**, *6*, 1515–1524.

[14] a) Y. Shichibu, Y. Negishi, T. Watanabe, N. K. Chaki, H. Kawaguchi, T. Tsukuda, *J. Phys. Chem. C* **2007**, *111*, 7845–7847; b) M. W. Heaven, A. Dass, P. S. White, K. M. Holt, R. W. Murray, *J. Am. Chem. Soc.* **2008**, *130*, 3754–3755; c) M. Zhu, C. M. Aikens, F. J. Hollander, G. C. Schatz, R. Jin, *J. Am. Chem. Soc.* **2008**, *130*, 5883–5885; d) M. Z. Zhu, W. T. Eckenhoff, T. Pintauer, R. C. Jin, *J. Phys. Chem. C* **2008**, *112*, 14221–14224; e) T. Dainese, S. Antonello, J. A. Gascón, F. Pan, N. V. Perera, M. Ruzzi, A. Venzo, A. Zoleo, K. Rissanen, F. Maran, *ACS Nano* **2014**, *8*, 3904–3912; f) M. De Nardi, S. Antonello, D. E. Jiang, F. F. Pan, K. Rissanen, M. Ruzzi, A. Venzo, A. Zoleo, F. Maran, *ACS Nano* **2014**, *8*, 8505–8512; g) G. A. Simms, J. D. Padmos, P. Zhang, *J. Chem. Phys.* **2009**, *131*, 214703.

[15] K. Chaudhari, P. L. Xavier, T. Pradeep, *ACS Nano* **2011**, *5*, 8816–8827.

[16] X. Le Guevel, B. Hotzer, G. Jung, K. Hollemeyer, V. Trouillet, M. Schneider, *J. Phys. Chem. C* **2011**, *115*, 10955–10963.

[17] a) N. Fernandez-Iglesias, J. Bettmer, *Nanoscale* **2014**, *6*, 716–721; b) Y. Yue, T. Y. Liu, H. W. Li, Z. Liu, Y. Wu, *Nanoscale* **2012**, *4*, 2251–2254.

[18] Y. Yu, Z. Luo, C. S. Teo, Y. N. Tan, J. Xie, *Chem. Commun.* **2013**, *49*, 9740–9742.

[19] a) J. P. Xie, Y. G. Zheng, J. Y. Ying, *Chem. Commun.* **2010**, *46*, 961–963; b) H. Y. Liu, X. A. Zhang, X. M. Wu, L. P. Jiang, C. Burda, J. J. Zhu, *Chem. Commun.* **2011**, *47*, 4237–4239; c) Y. He, X. Wang, J. J. Zhu, S. H. Zhong, G. W. Song, *Analyst* **2012**, *137*, 4005–4009.

[20] a) Y. L. Liu, K. L. Ai, X. L. Cheng, L. H. Huo, L. H. Lu, *Adv. Funct. Mater.* **2010**, *20*, 951–956; b) M. L. Cui, J. M. Liu, X. X. Wang, L. P. Lin, L. Jiao, Z. Y. Zheng, L. H. Zhang, S. L. Jiang, *Sens. Actuators B* **2013**, *188*, 53–58; c) B. Unnikrishnan, S. C. Wei, W. J. Chiu, J. Cang, P. H. Hsu, C. C. Huang, *Analyst* **2014**, *139*, 2221–2228; d) R. P. Li, P. P. Xu, J. Fan, J. W. Di, Y. F. Tu, J. L. Yan, *Anal. Chim. Acta* **2014**, *827*, 80–85.

[21] a) L. H. Jin, L. Shang, S. J. Guo, Y. X. Fang, D. Wen, L. Wang, J. Y. Yin, S. J. Dong, *Biosens. Bioelectron.* **2011**, *26*, 1965–1969; b) X. X. Wang, P. Wu, Y. Lv, X. D. Hou, *Microchem. J.* **2011**, *99*, 327–331; c) F. Samari, B. Hemmateenejad, Z. Rezaei, M. Shamsipur, *Anal. Methods* **2012**, *4*, 4155–4160; d) B. Hemmateenejad, F. Shakerizadeh-shirazi, F. Samari, *Sens. Actuators B* **2014**, *199*, 42–46; e) X. X. Wang, P. Wu, X. D. Hou, Y. Lv, *Analyst* **2013**, *138*, 229–233; f) X. Yang, J. H. Wang, D. Y. Su, Q. D. Xia, F. Chai, C. G. Wang, F. Y. Qu, *Dalton Trans.* **2014**, *43*, 10057–10063.

[22] Z. G. Chen, S. H. Qian, X. Chen, W. H. Gao, Y. J. Lin, *Analyst* **2012**, *137*, 4356–4361.

[23] E. G. Ju, Z. Liu, Y. D. Du, Y. Tao, J. S. Ren, X. G. Qu, *ACS Nano* **2014**, *8*, 6014–6023.

[24] L. Z. Hu, S. Han, S. Parveen, Y. L. Yuan, L. Zhang, G. B. Xu, *Biosens. Bioelectron.* **2012**, *32*, 297–299.

[25] C. M. Hofmann, J. B. Essner, G. A. Baker, S. N. Baker, *Nanoscale* **2014**, *6*, 5425–5431.

[26] D. H. Tian, Z. S. Qian, Y. S. Xia, C. Q. Zhu, *Langmuir* **2012**, *28*, 3945–3951.

[27] B. Aswathy, G. Sony, *Microchem. J.* **2014**, *116*, 151–156.

[28] Z. G. Chen, G. M. Zhang, X. Chen, J. H. Chen, J. B. Liu, H. Q. Yuan, *Biosens. Bioelectron.* **2013**, *41*, 844–847.

[29] H. C. Li, Y. X. Guo, L. H. Xiao, B. Chen, *Biosens. Bioelectron.* **2014**, *59*, 289–292.

[30] H. W. Li, Y. Yue, T. Y. Liu, D. M. Li, Y. Q. Wu, *J. Phys. Chem. C* **2013**, *117*, 16159–16165.

[31] a) B. Paramanik, S. Bhattacharyya, A. Patra, *Chem. Eur. J.* **2013**, *19*, 5980–5987; b) M. L. Cui, J. M. Liu, X. X. Wang, L. P. Lin, L. Jiao, L. H. Zhang, Z. Y. Zheng, S. Q. Lin, *Analyst* **2012**, *137*, 5346–5351.

[32] a) H. Wei, E. Wang, *Anal. Chem.* **2008**, *80*, 2250–2254; b) H. Wei, E. K. Wang, *Chem. Soc. Rev.* **2013**, *42*, 6060–6093.

[33] a) X. X. Wang, Q. Wu, Z. Shan, Q. M. Huang, *Biosens. Bioelectron.* **2011**, *26*, 3614–3619; b) D. H. Hu, Z. H. Sheng, S. T. Fang, Y. A. Wang, D. Y. Gao, P. F. Zhang, P. Gong, Y. F. Ma, L. T. Cai, *Theranostics* **2014**, *4*, 142–153.

[34] a) J. Peng, L. N. Feng, K. Zhang, X. H. Li, L. P. Jiang, J. J. Zhu, *Chem. Eur. J.* **2012**, *18*, 5261–5268; b) H. Y. Liu, X. M. Wu, X. Zhang, C. Burda, J. J. Zhu, *J. Phys. Chem. C* **2012**, *116*, 2548–2554.

[35] a) Y. Du, H. Wei, J. Z. Kang, J. L. Yan, X. B. Yin, X. R. Yang, E. K. Wang, *Anal. Chem.* **2005**, *77*, 7993–7997; b) H. Wei, E. Wang, *Chem. Lett.* **2007**, *36*, 210–211; c) L. Y. Fang, Z. Z. Lv, H. Wei, E. Wang, *Anal. Chim. Acta* **2008**, *628*, 80–86; d) H. Wei, J. Y. Yin, E. Wang, *Anal. Chem.* **2008**, *80*, 5635–5639; e) J. Li, Y. H. Xu, H. Wei, T. Huo, E. K. Wang, *Anal. Chem.* **2007**, *79*, 5439–5443; f) H. Wei, Y. Du, J. Z. Kang, E. K. Wang, *Electrochem. Commun.* **2007**, *9*, 1474–1479; g) H. Wei, J. Liu, L. Zhou, J. Li, X. Jiang, J. Kang, X. Yang, S. Dong, E. Wang, *Chem. Eur. J.* **2008**, *14*, 3687–3693; h) L. Y. Fang, Z. Z. Lu, H. Wei, E. K. Wang, *Biosens. Bioelectron.* **2008**, *23*, 1645–1651; i) H. Wei, L. L. Zhou, J. Li, J. F. Liu, E. K. Wang, *J. Colloid Interface Sci.* **2008**, *321*, 310–314; j) H. Wei, E. Wang, *Luminescence* **2011**, *26*, 77–85; k) H. Wei, E. Wang, *TrAC Trends Anal. Chem.* **2008**, *27*, 447–459; l) J. Bai, H. Wei, B. Li, L. Song, L. Fang, Z. Lv, W. Zhou, E. Wang, *Chem. Asian J.* **2008**, *3*, 1935–1941.

[36] a) L. L. Li, H. Y. Liu, Y. Y. Shen, J. R. Zhang, J. J. Zhu, *Anal. Chem.* **2011**, *83*, 661–665; b) Y. M. Fang, J. Song, J. A. Li, Y. W. Wang, H. H. Yang, J. J. Sun, G. N. Chen, *Chem. Commun.* **2011**, *47*, 2369–2371.

[37] a) X. Chen, J. B. Essner, G. A. Baker, *Nanoscale* **2014**, *6*, 9594–9598; b) L. P. Zhang, M. Zhang, Y. Q. Wu, *J. Mol. Struct.* **2014**, *1069*, 245–250.

[38] a) S. L. Raut, R. Fudala, R. Rich, R. A. Kokate, R. Chib, Z. Gryczynski, I. Gryczynski, *Nanoscale* **2014**, *6*, 2594–2597; b) Y. L. Wang, J. J. Chen, J. Irudayaraj, *ACS Nano* **2011**, *5*, 9718–9725; c) S. K. Sun, L. X. Dong, Y. Cao, H. R. Sun, X. P. Yan, *Anal. Chem.* **2013**, *85*, 8436–8441; d) E. S. Shibu, S. Sugino, K. Ono, H. Saito, A. Nishioka, S. Yamamura, M. Sawada, Y. Nosaka, V. Biju, *Angew. Chem. Int. Ed.* **2013**, *52*, 10559–10563; e) G. Y. Sun, L. Zhou, Y. L. Liu, Z. B. Zhao, *New J. Chem.* **2013**, *37*, 1028–1035; f) Y. Osakada, G. Pratx, C. Sun, M. Sakamoto, M. Ahmad, O. Volotskova, Q. X. Ong, T. Teranishi, Y. Harada, L. Xing, B. X. Cui, *Chem. Commun.* **2014**, *50*, 3549–3551; g) Z. J. Zhou, C. L. Zhang, Q. R. Qian, J. B. Ma, P. Huang, X. Zhang, L. Y. Pan, G. Gao, H. L. Fu, S. Fu, H. Song, X. Zhi, J. Ni, D. X. Cui, *J. Nanobiotechnol.* **2013**, *11*, 17; h) D. H. Hu, Z. H. Sheng, P. F. Zhang, D. Z. Yang, S. H. Liu, P. Gong, D. Y. Gao, S. T. Fang, Y. F. Ma, L. T. Cai, *Nanoscale* **2013**, *5*, 1624–1628; i) S. S. Su, H. Wang, X. G. Liu, Y. Wu, G. J. Nie, *Biomaterials* **2013**, *34*, 3523–3533; j) A. L. Zhang, Y. Tu, S. B. Qin, Y.

Li, J. Y. Zhou, N. Chen, Q. Lu, B. B. Zhang, *J. Colloid Interface Sci.* **2012**, *372*, 239–244; k) A. Retnakumari, S. Setua, D. Menon, P. Ravindran, H. Muhammed, T. Pradeep, S. Nair, M. Koyakutty, *Nanotechnology* **2010**, *21*, 055103.

[39] S. L. Raut, D. Shumilov, R. Chib, R. Rich, Z. Gryczynski, I. Gryczynski, *Chem. Phys. Lett.* **2013**, *561*, 74–76.

[40] a) A. Mathew, P. R. Sajanlal, T. Pradeep, *J. Mater. Chem.* **2011**, *21*, 11205–11212; b) D. T. Lu, C. H. Zhang, L. Fan, H. J. Wu, S. M. Shuang, C. Dong, *Anal. Methods* **2013**, *5*, 5522–5527; c) A. S. Patel, T. Mohanty, *J. Mater. Sci.* **2014**, *49*, 2136–2143; d) X. H. Yang, J. Ling, J. Peng, Q. E. Cao, L. Wang, Z. T. Ding, J. Xiong, *Spectrochim. Acta Part A* **2013**, *106*, 224–230; e) T. Liu, L. C. Zhang, H. J. Song, Z. H. Wang, Y. Lv, *Luminescence* **2013**, *28*, 530–535.

[41] a) L. Z. Hu, Y. L. Yuan, L. Zhang, J. M. Zhao, S. Majeed, G. B. Xu, *Anal. Chim. Acta* **2013**, *762*, 83–86; b) Z. Gao, R. X. Su, W. Qi, L. B. Wang, Z. M. He, *Sens. Actuators B* **2014**, *195*, 359–364; c) C. Wang, C. X. Wang, L. Xu, H. Cheng, Q. Lin, C. Zhang, *Nanoscale* **2014**, *6*, 1775–1781.

[42] W. Y. Chen, J. Y. Lin, W. J. Chen, L. Y. Luo, E. W. G. Diau, Y. C. Chen, *Nanomedicine* **2010**, *5*, 755–764.

[43] a) J. M. Liu, J. T. Chen, X. P. Yan, *Anal. Chem.* **2013**, *85*, 3238–3245; b) W. Wang, F. Leng, L. Zhan, Y. Chang, X. X. Yang, J. Lan, C. Z. Huang, *Analyst* **2014**, *139*, 2990–2993; c) P. C. Liu, L. Shang, H. W. Li, Y. X. Cui, Y. M. Qin, Y. Q. Wu, J. K. Hiltunen, Z. J. Chen, J. C. Shen, *RSC Adv.* **2014**, *4*, 31536–31543; d) H. Kawasaki, K. Hamaguchi, I. Osaka, R. Arakawa, *Adv. Funct. Mater.* **2011**, *21*, 3508–3515; e) Y. Chen, Y. Wang, C. X. Wang, W. Y. Li, H. P. Zhou, H. P. Jiao, Q. Lin, C. Yu, *J. Colloid Interface Sci.* **2013**, *396*, 63–68; f) Y. F. Kong, J. Chen, F. Gao, R. Brydson, B. Johnson, G. Heath, Y. Zhang, L. Wu, D. J. Zhou, *Nanoscale* **2013**, *5*, 1009–1017; g) A. L. West, M. H. Griep, D. P. Cole, S. P. Karna, *Anal. Chem.* **2014**, *86*, 7377–7382.

[44] L. Yan, Y. Q. Cai, B. Z. Zheng, H. Y. Yuan, Y. Guo, D. Xiao, M. M. F. Choi, *J. Mater. Chem.* **2012**, *22*, 1000–1005.

[45] P. H. Chan, Y. C. Chen, *Anal. Chem.* **2012**, *84*, 8952–8956.

[46] S. Ghosh, U. Anand, S. Mukherjee, *Anal. Chem.* **2014**, *86*, 3188–3194.

[47] U. Anand, S. Ghosh, S. Mukherjee, *J. Phys. Chem. Lett.* **2012**, *3*, 3605–3609.

[48] a) S. M. Lystvet, S. Volden, G. Singh, M. Yasuda, O. Halskau, W. R. Glomm, *RSC Adv.* **2013**, *3*, 482–495; b) Y. Tao, E. G. Ju, Z. H. Li, J. S. Ren, X. G. Qu, *Adv. Funct. Mater.* **2014**, *24*, 1004–1010; c) K. Selvaprakash, Y. C. Chen, *Biosens. Bioelectron.* **2014**, *61*, 88–94.

[49] C. Y. Shao, B. Yuan, H. Q. Wang, Q. A. Zhou, Y. L. Li, Y. F. Guan, Z. X. Deng, *J. Mater. Chem.* **2011**, *21*, 2863–2866.

[50] a) C. J. Sun, H. Yang, Y. Yuan, X. Tian, L. M. Wang, Y. Guo, L. Xu, J. L. Lei, N. Gao, G. J. Anderson, X. J. Liang, C. Y. Chen, Y. L. Zhao, G. J. Nie, *J. Am. Chem. Soc.* **2011**, *133*, 8617–8624; b) Y. Wang, J.-T. Chen, X.-P. Yan, *Anal. Chem.* **2013**, *85*, 2529–2535; c) F. Wen, Y. H. Dong, L. Feng, S. Wang, S. C. Zhang, X. R. Zhang, *Anal. Chem.* **2011**, *83*, 1193–1196; d) N. Goswami, A. Baksi, A. Giri, P. L. Xavier, G. Basu, T. Pradeep, S. K. Pal, *Nanoscale* **2014**, *6*, 1848–1854; e) C. L. Liu, H. T. Wu, Y. H. Hsiao, C. W. Lai, C. W. Shih, Y. K. Peng, K. C. Tang, H. W. Chang, Y. C. Chien, J. K. Hsiao, J. T. Cheng, P. T. Chou, *Angew. Chem. Int. Ed.* **2011**, *50*, 7056–7060; f) D. Joseph, K. E. Geckeler, *Colloids Surf. B* **2014**, *115*, 46–50; g) X. Le Guevel, N. Daum, M. Schneider, *Nanotechnology* **2011**, *22*, 275103; h) P. L. Xavier, K. Chaudhari, P. K. Verma, S. K. Pal, T. Pradeep, *Nanoscale* **2010**, *2*, 2769–2776.

[51] a) S. Choi, R. M. Dickson, J.-K. Lee, J. Yu, *Photochem. Photobiol. Sci.* **2012**, *11*, 274–278; b) J. Wang, J. Ye, H. Jiang, S. Gao, W. Ge, Y. Chen, C. Liu, C. Amatore, X. Wang, *RSC Adv.* **2014**, *4*, 37790–37795.

[52] S. Volden, S. M. Lystvet, O. Halskau, W. R. Glomm, *RSC Adv.* **2012**, *2*, 11704–11711.

[53] a) C. L. Chen, N. L. Rosi, *Angew. Chem. Int. Ed.* **2010**, *49*, 1924–1942; b) C. Y. Chiu, L. Y. Ruan, Y. Huang, *Chem. Soc. Rev.* **2013**, *42*, 2512–2527.

[54] a) T. G. Schaaff, G. Knight, M. N. Shafigullin, R. F. Borkman, R. L. Whetten, *J. Phys. Chem. B* **1998**, *102*, 10643–10646; b) T. G. Schaaff, R. L. Whetten, *J. Phys. Chem. B* **2000**, *104*, 2630–2641.

[55] Y. Negishi, K. Nobusada, T. Tsukuda, *J. Am. Chem. Soc.* **2005**, *127*, 5261–5270.

[56] Z. Luo, X. Yuan, Y. Yu, Q. Zhang, D. T. Leong, J. Y. Lee, J. Xie, *J. Am. Chem. Soc.* **2012**, *134*, 16662–16670.

[57] a) Y. Yu, X. Chen, Q. Yao, Y. Yu, N. Yan, J. Xie, *Chem. Mater.* **2013**, *25*, 946–952; b) Q. Yao, Y. Yu, X. Yuan, Y. Yu, J. Xie, J. Y. Lee, *Small* **2013**, *9*, 2696–2701.

[58] G. Zhang, Y. Li, J. Xu, C. Zhang, S. Shuang, C. Dong, M. M. F. Choi, *Sens. Actuators B* **2013**, *183*, 583–588.

[59] T. Chen, Y. Hu, Y. Cen, X. Chu, Y. Lu, *J. Am. Chem. Soc.* **2013**, *135*, 11595–11602.

[60] a) J. Liu, M. Yu, C. Zhou, S. Yang, X. Ning, J. Zheng, *J. Am. Chem. Soc.* **2013**, *135*, 4978–4981; b) X.-D. Zhang, D. Wu, X. Shen, P.-X. Liu, F.-Y. Fan, S.-J. Fan, *Biomaterials* **2012**, *33*, 4628–4638.

[61] C. Zhou, M. Long, Y. Qin, X. Sun, J. Zheng, *Angew. Chem. Int. Ed.* **2011**, *50*, 3168–3172.

[62] R. D. Vinluan, III, J. Liu, C. Zhou, M. Yu, S. Yang, A. Kumar, S. Sun, A. Dean, X. Sun, J. Zheng, *ACS Appl. Mater. Interfaces* **2014**, *6*, 11829–11833.

[63] X. D. Zhang, J. Chen, Z. T. Luo, D. Wu, X. Shen, S. S. Song, Y. M. Sun, P. X. Liu, J. Zhao, S. D. Huo, S. J. Fan, F. Y. Fan, X. J. Liang, J. P. Xie, *Adv. Healthcare Mater.* **2014**, *3*, 133–141.

[64] a) C. Zhang, Z. Zhou, Q. Qian, G. Gao, C. Li, L. Feng, Q. Wang, D. Cui, *J. Mater. Chem. B* **2013**, *1*, 5045–5053; b) O. A. Wong, R. J. Hansen, T. W. Ni, C. L. Heinecke, W. S. Compel, D. L. Gustafson, C. J. Ackerson, *Nanoscale* **2013**, *5*, 10525–10533.

[65] X. Yuan, M. I. Setyawati, A. S. Tan, C. N. Ong, D. T. Leong, J. Xie, *NPG Asia Mater.* **2013**, *5*, e39.

[66] F. Bertorelle, R. Hamouda, D. Rayane, M. Broyer, R. Antoine, P. Dugourd, L. Gell, A. Kulesza, R. Mitric, V. Bonacic-Koutecky, *Nanoscale* **2013**, *5*, 5637–5643.

[67] X. Le Guevel, C. Spies, N. Daum, G. Jung, M. Schneider, *Nano Res.* **2012**, *5*, 379–387.

[68] S. Roy, A. Baral, A. Banerjee, *ACS Appl. Mater. Interfaces* **2014**, *6*, 4050–4056.

[69] I. Chakraborty, T. Udayabhaskararao, G. K. Deepesh, T. Pradeep, *J. Mater. Chem. B* **2013**, *1*, 4059–4064.

[70] X. Le Guevel, V. Trouillet, C. Spies, G. Jung, M. Schneider, *J. Phys. Chem. C* **2012**, *116*, 6047–6051.

[71] M. Ganguly, C. Mondal, J. Pal, A. Pal, Y. Negishi, T. Pal, *Dalton Trans.* **2014**, *43*, 11557–11565.

[72] a) P. Yu, X. Wen, Y.-R. Toh, J. Tang, *J. Phys. Chem. C* **2012**, *116*, 6567–6571; b) B. Adhikari, A. Banerjee, *Chem. Eur. J.* **2010**, *16*, 13698–13705.

[73] B. Soptei, L. N. Nagy, P. Baranyai, I. Szabo, G. Mezo, F. Hudecz, A. Bota, *Gold Bull.* **2013**, *46*, 195–203.

[74] Y. Wang, Y. Cui, R. Liu, Y. Wei, X. Jiang, H. Zhu, L. Gao, Y. Zhao, Z. Chai, X. Gao, *Chem. Commun.* **2013**, *49*, 10724–10726.
[75] Y. L. Wang, Y. Y. Cui, Y. L. Zhao, R. Liu, Z. P. Sun, W. Li, X. Y. Gao, *Chem. Commun.* **2012**, *48*, 871–873.
[76] R. de la Rica, L. W. Chow, C.-M. Horejs, M. Mazo, C. Chiappini, E. T. Pashuck, R. Bitton, M. M. Stevens, *Chem. Commun.* **2014**, *50*, 10648–10650.
[77] G. Liang, D. Ye, X. Zhang, F. Dong, H. Chen, S. Zhang, J. Li, X. Shen, J. Kong, *J. Mater. Chem. B* **2013**, *1*, 3545–3552.
[78] J. Yu, S. A. Patel, R. M. Dickson, *Angew. Chem. Int. Ed.* **2007**, *46*, 2028–2030.
[79] Q. Wen, Y. Gu, L.-J. Tang, R.-Q. Yu, J.-H. Jiang, *Anal. Chem.* **2013**, *85*, 11681–11685.
[80] a) P. Wu, Y. Yu, C. E. McGhee, L. H. Tan, Y. Lu, *Adv. Mater.* **2014**, *26*, 7849–7872; b) T. Tabarin, A. Kulesza, R. Antoine, R. Mitric, M. Broyer, P. Dugourd, V. Bonacic-Koutecky, *Phys. Rev. Lett.* **2008**, *101*, 213001.
[81] V. A. Morozov, M. Y. Ogawa, *Inorg. Chem.* **2013**, *52*, 9166–9168.
[82] Z. Wu, R. Jin, *ACS Nano* **2009**, *3*, 2036–2042.
[83] J. Li, X. Li, H.-J. Zhai and L.-S. Wang, *Science*, **2003**, *229*, 864–867.
[84] B. Fresch, H.-G. Boyenbc, F. Remacle, *Nanoscale*, **2012**, *4*, 4138–4147.
[85] C.-P. Liu, T.-H. Wu, C.-Y. Liu, H.-J. Cheng, S.-Y. Lin, *J. Mater. Chem. B*, **2015**, *3*, 191–197.

Received: November 12, 2014
Accepted: January 5, 2015
Published online: March 27, 2015